A Comparative Study of Different Modeling Tools and Analysis Techniques for Aeroelastic Stability Assessment

To cite this article: S Cacciola *et al* 2026 *J. Phys.: Conf. Ser.* **3224** 042028

A Comparative Study of Different Modeling Tools and Analysis Techniques for Aeroelastic Stability Assessment

S Cacciola[1], A Croce[1], G Bangga[2], G Pirrung[3], N Bonfils[4], L Greco[5], N Aryan[6], A Castorrini[6], V Morici[6], M Chetan[7], J Jonkman[7], E Branlard[8], S Cherubini[9], C Bernardi[9], K Boorsma[10], J G Schepers[10], F J Savenije[10], A Bianchini[11], L Pagamonci[11], F Papi[11], O Hach[12], M Imiela[12], D. Witt[12].

[1]Department of Aerospace Science and Technology, Politecnico di Milano, Milan, Italy
[2]DNV, Bristol, UK
[3]DTU, Roskilde, DK
[4]IFPEN, Rueil-Malmaison, France
[5]CNR-INM, Rome, Italy
[6]Sapienza Università di Roma, Rome, Italy
[7]National Laboratory of the Rockies, Colorado, USA
[8]University of Massachusetts, Amherst, USA
[9]Politecnico di Bari, Bari, Italy
[10]TNO, Petten, The Netherlands
[11]Università degli studi di Firenze, Florence, Italy
[12]DLR, Braunschweig, Germany

E-mail: `stefano.cacciola@polimi.it`

Abstract. Modern simulation and analysis tools rely on assumptions and numerical schemes that inevitably affect their outputs, leading to uncertainties and biases that must be quantified and bounded, especially when they influence critical aspects such as system stability. This paper presents recent results from an aeroelastic benchmark on a reference 15-MW wind turbine, conducted by multiple partners within the framework of the International Energy Agency (IEA) Wind TCP Task 47 TURBINIA, focusing on stability characteristics and aeroelastic responses. The agreement among the results is reasonably good, although some quantities exhibit a significant spread. This is particularly evident in the damping factors of the turbine modes and in the periodic loads observed under sheared conditions.

1. Introduction

As wind turbines grow in size, the accuracy of modeling, analysis, and performance evaluation tools becomes increasingly important. Key challenges include large structural deflections, nonstationary aerodynamics, and complex interactions among structures, aerodynamics, and controls. All assumptions and integration schemes implemented in modern and sophisticated simulators impact their output such that numerical investigations carry uncertainty and biases that must be quantified and bounded, especially when they affect system stability and resilience.

Different simulators and numerical procedures are typically compared in large benchmarks, where various cases are simulated and results analyzed. These benchmarks help detect modeling errors and assess the influence of different procedures on turbine performance. For wind turbines, modal analysis requires special attention. In fact, rotating machines exhibit periodic behavior even under idealized conditions, such as in vacuo without gravity. For example, tower–rotor interaction introduces periodicity, resulting in whirling modes [1]. Stability analysis of such systems is typically performed through advanced methods, such as Coleman transformation [2], system identification [3], or simplified Floquet analysis [4]. These approaches involve approximations and limitations, highlighting the need for benchmarking stability procedures.

A relevant benchmark focused on the aeroelastic behavior of the rotor of a 22-MW reference turbine is presented in [5], considering four wind turbine simulators. The analysis in [5] was mainly focused on rotor behavior, as it often included a rigid tower model.

The work presented in this paper aims to provide an assessment of the discrepancies that characterize the outputs of aeroelastic analyses of large-scale and highly flexible wind turbine, with an emphasis on the evaluation of stability characteristics and aeroelastic responses. This benchmark was conducted within the framework of IEA Wind TCP Task 47 TURBINIA [6].

The wind energy community may benefit from this work in multiple ways. First, the present comparison offers a quantitative evaluation of the variability that may characterize the outputs of modern state-of-the-art simulation and analysis tools, typically employed for turbine design and research purposes. Second, it introduces a scheme to benchmark aeroelastic solvers and their stability assessment procedures. This framework represents an enhanced version of an analogous scheme employed in [7].

2. Description of the comparative analyses

All cases were conducted on the reference IEA 15-MW wind turbine [8]. In the whole comparison, the controller was ignored and the pitch settings and rotor speed were considered known functions of the inflow speed, as defined in Sec. 2.1. Due to the complex structure and significant rotor flexibility, we decided to replace the nominal blade with a simpler one with the same aerodynamic properties but different internal properties. The simpler blade, hereafter indicated with "*simplified*", features diagonal sectional stiffness matrices (all cross-coupling terms are zeroed), while the nominal model, characterized by all couplings arising due to full 6×6 sectional stiffness, is indicated with "*full*" model.

The goal of the comparative analysis is to benchmark different wind turbine analysis codes in terms of their aeroelastic behavior, including both response to steady wind conditions and turbine modal frequencies and damping factors.

To have a comprehensive evaluation and possibly find the origin of significant discrepancies, different tests of increasing complexity, ranging from isolated blade frequency computation to full-system dynamic simulations, have been proposed to partners. Gradually increasing the complexity of the considered scenarios has the clear advantage of allowing one to detect possible inconsistencies in the modeling of turbine sub-components. After verifying the correctness of the turbine assembly, which comprises both the sub-components and their coupling, it is possible to finally assess the accuracy of the stability analysis tools for the evaluation of the damping factors of interest and for verifying the proximity of flutter boundaries.

The benchmarked simulation tools are listed in Tab. 1. The table reports, in the first column, the partner name and, in brackets, the abbreviation that will be used to indicate the corresponding results in all plots. The second column displays the name of the employed tool. In the column "Aerodynamic implementation", the model adopted to represent the turbine aerodynamics is indicated, with "BEM" and "LES", referring respectively to the widely used Blade Element Momentum and Large Eddy Simulation. The structural models employed by all partners are reported in the fourth column to clarify the structural implementation used by the partners. In particular, “GEBT” indicates non-linear geometrical exact beam models, “Lumped” refers to a particular formulation where all blade segments are treated as rigid and connected each other through springs and dampers modeling the flap, lag and torsional flexibility. The “3D FEM”, indicated on the line of partner UniRoma, refers to a full three-dimensional shell-based structural model derived from a CAD representation of the blade. The last column indicates the methodology adopted to perform the periodic stability analysis of the rotating turbine. Both “Coleman-based” and “Identification-based” methodologies will be described in Sec. 3.2. Obviously, Tab. 1 cannot be exhaustive in capturing all possible differences in various simulators. For a detailed description of the individual tools, the reader is referred to the IEA Task 29 and Task 47 reports [6, 7].

Table 1. Partner and simulation code definitions

Partner	Code name	Aerodynamic implementation	Structural model	Periodic stability type
DLR	Simpack	BEM	Timoshenko	Coleman
DNV	Bladed	BEM	FEM	Coleman
DTU	HAWC2 and HAWC2Stab	BEM	Timoshenko	Coleman
IFPEN	Deeplines Wind and AeroDeeP	BEM	Timoshenko	n.a.
CNR-INM	AEOLIAN	BEM	Lumped	n.a.
NLR	OpenFAST	BEM	GEBT	Coleman
Politecnico di Bari (PoliBari)	UTD-WF	LES	FEM	n.a.
Politecnico di Milano (PoliMI)	Cp-Lambda	BEM	GEBT	Identification
TNO	Phatas	BEM	GEBT	n.a.
Università degli Studi di Firenze (UniFI)	CALMA-Tool	BEM	Modal	Coleman
La Sapienza (UniRoma)	APDL	n.a.	3D FEM	n.a.
La Sapienza (UniRoma)	in-house FEM	n.a.	FEM	n.a.

2.1. Aeroelastic simulations and modal analyses
For this benchmark, the following cases have been considered:

(i) Computation of the natural frequencies and damping factors of the isolated blade. This case considers “*full*” and “*simplified*” blades, without considering aerodynamics and gravity. The goal of this analysis is to understand how different tools predict the modal data of a complex structure, where twist, prebend and the couplings introduced in the structural design create multiple interactions among flap, lag, and torsional degrees of freedom.

(ii) Computation of the natural frequencies and damping factors of the isolated tower, rigidly clamped to the ground, without the rotor-nacelle assembly. This simple analysis is used for detecting possible inconsistencies in the modeling construction. The agreement of the isolated tower modes is comparable to that obtained for the first blade mode. For this reason, and for the sake of brevity, the tower analysis is not reported in this paper.

(iii) Derivation of the Campbell diagram of the entire turbine, *in vacuo* and in air. This task was considered only for the "*simplified*" model. The stability analysis, needed to draw the Campbell diagram, was conducted for different wind speed values from cut-in to cut-out, with blade pitch angles and rotor speed values selected according to the control trim set points reported in Tab. 2. Analyses *in vacuo*, i.e. excluding the aerodynamics, are essential to characterize the structural damping of the entire turbine, which represents a factor of paramount importance in the proximity of the flutter boundaries, i.e. when the aerodynamic damping is small or even slightly negative. On the other hand, the analyses in the air represent the core stability assessment.

Table 2. Conditions for Campbell diagram derivation. Data were extracted from [8].

Wind speed [m/s]	7.5	9.0	10.9	17.0	25.0
Omega [RPM]	5.33	6.39	7.5	7.5	7.5
Pitch angle [deg]	0.0	0.0	0.0	13.95	22.69

(iv) Dynamic simulations in Nominal Wind Profile (NWP) conditions. For the same set points listed in Tab. 2, dynamic simulations were performed without the control system by fixing rotor speed and collective pitch angle. The inflow was set according to a Normal Wind Profile, i.e. exponential wind shear with $\alpha = 0.2$, excluding turbulence and yaw misalignment. Both blade models, "*simplified*" and "*full*", were analyzed. Due to the presence of shear and gravity, the turbine response is periodic. Accordingly, the comparison considers the mean values of specific outputs and the related periodic components at the rotational frequency (1p). The analyzed measurements include rotor thrust (`HCR Fx`), side-side and fore-aft tower-base bending moments (`TB Mx` and `TB My`), blade-root pitchable edgewise and flapwise moment (`BRP Mx` and `BRP My`) and the amplitude and phase of the 1p oscillation of blade-root flap-wise moment. All measurements are defined following commonly used references [9].

3. Results

In this section, the most significant outputs of the comparison will be reported. Each subsection deals with a specific comparison round.

3.1. Modes of isolated blade

All partners provided the modal frequencies and the damping factors of the isolated blade, allowing the simplest comparison of the most important turbine component.

The frequency and damping factors of the isolated blade are shown in Fig. 1 and 2, respectively for the "*full*" and "*simplified*" model. The names of the modes are displayed on the x-axis.

From both figures, it is clear that the agreement in the frequencies is excellent for the first four modes (two flap-wise and two edge-wise). The spread characterizing these frequencies, computed as the ratio between the standard deviation and the mean value of the partners' outputs, is approximately 5% for the full model, and around 4% for the simplified blade. Modes #6 and #7, which are very close in frequency, exhibit a strong coupling between edge-wise and torsional degrees of freedom, making them difficult to distinguish. In the plot, they are therefore arranged in order of increasing frequency. Nevertheless, we may classify mode #6 as the third edge-wise mode and mode #7 as the torsional one. Both modes exhibit a higher, yet still acceptable, spread in the range 7%-10%. This may indicate a different formulation employed to render the torsional degrees of freedom within a pre-bended and twisted beam model. Although the matching is still acceptable, this aspect deserves further investigation as the torsion of the

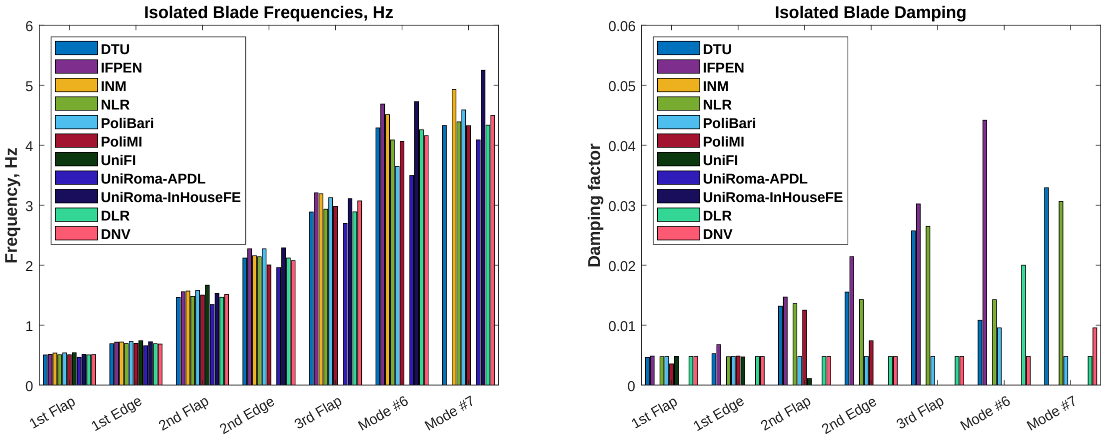

Figure 1. Frequencies and damping of the isolated blade (full model)

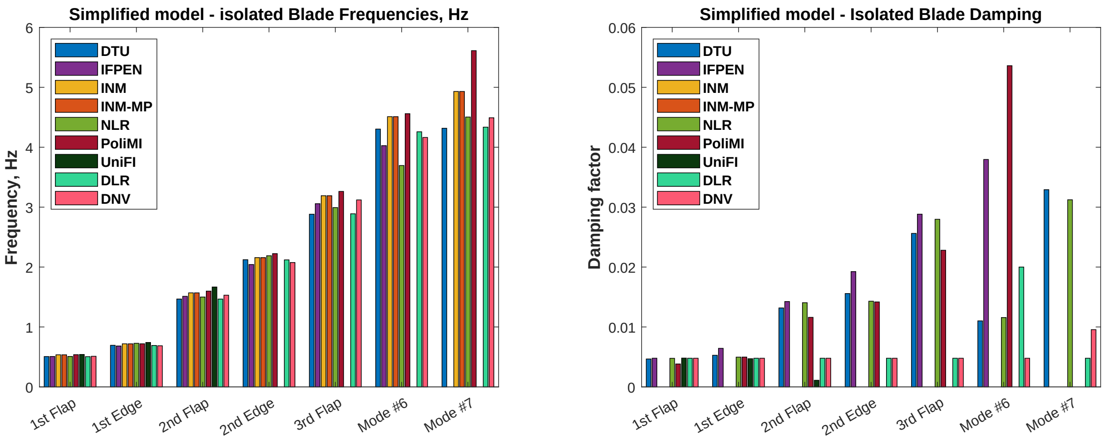

Figure 2. Frequencies and damping of the isolated blade (simplified model)

blade has a significant impact on the static performance of the rotor, even if the torsional mode is at a relatively high frequency.

Dealing with blade structural damping factors, there is a good agreement only for the first two blade modes (first flap and first edge). This fact is certainly due to the different implementations of the structural damping. For example, finite element-based beam models typically consider a sectional damping proportional to the stiffness (whereby damping increases with frequency), whereas modal condensation-based tools allow one to directly assign a modal damping to each mode independently, as also suggested in [8]. This represents an aspect that should be considered when assessing instability and flutter boundaries in simulated studies.

3.2. Campbell diagram of the entire turbine in vacuo *and in the air*
The Campbell diagram is a plot of the eigen-frequencies of a rotating system as functions of the rotor angular velocity, typically employed in rotor design. In wind turbine analysis, it is often plotted against wind speed, enabling system frequencies to be displayed in the full-power region, where the rotor speed remains constant while the collective pitch varies.

The analyses considered in the derivation of the Campbell diagram must account for the turbine periodic nature, caused by gravity, shear, misalignment, and tower–rotor interaction.

For example, the whirling modes can be explained through the mutual interaction between tower and rotor, even excluding the presence of aerodynamics and gravity [1]. Direct application of the rigorous periodic Floquet theory to whole turbine models is typically avoided due to its high computational cost and limited applicability to large multibody models. Instead, partners used methods based on linearization and Coleman transformation [2] (NLR, DTU, UniFI, DLR and DNV) or system identification [3] (Polimi).

The Coleman-based approach considers a linearized version of the system about a steady periodic trajectory and converts it to multiblade coordinates using a known periodic transformation. For rotors with three or more blades, the periodic content of system matrices is greatly reduced and can be removed by azimuth-averaging or selecting a representative azimuth. The resulting time-invariant model is analyzed with standard LTI techniques, such as the Arnoldi iteration for solving the eigen-problem, which efficiently extracts the first turbine modes. See [2, 3] for details. While not rigorously proven, practice shows that Coleman-based methods yield accurate frequency and damping estimates, however azimuth-averaging works well for low-order models (e.g., ElastoDyn in OpenFAST) but fails for high-order models (e.g., BeamDyn) due to sensitivity to small numerical errors.

Conversely, identification-based approaches consider reduced-order linear time-periodic I/O models (e.g., PARX type [3, 10]) fitted to simulated data. The full Floquet theory is then applied to the reduced system, yielding the modes of interest. The resulting procedure is model-independent and does not require linearizing the system. However, its accuracy depends on the quality of the identified model and, in turn, on the non-trivial design of the perturbations to excite relevant modes. Additionally, highly damped modes, often absent in the free response, are not captured. At present, although a full cross-validation of the two approaches is interesting for an overall assessment, such a comparison is not yet available in the literature. Figure 3 and 4 display the tower modes (side-side and fore-aft) and the first in-plane modes (collective, backward, and forward whirling modes) of the turbine in vacuo. The wind speed is used here as the independent variable to refer to the rotor speed and pitch angle indicated in Tab 2. Frequencies and damping factors are displayed respectively in the upper and bottom plots.

Although all partners' predictions capture the general behavior of the different modes, the spread in the results is quite visible. Since the agreement observed for the isolated sub-components (i.e. blade and tower) is satisfactory, at least in the low frequency range, the mismatch in the full turbine modes can most likely be attributed to the analysis processes that are not trivial for rotating systems with many DoFs, even if rotor aerodynamics are not included. For example, Coleman-based analyses rely on system linearization and azimuth-averaging of the Coleman-transformed system, which may introduce small errors, especially for highly flexible turbines featuring important nonlinearities due to large displacements. Moreover, analyses based on system identification, although potentially capable of capturing the full periodic nature of turbine dynamics, are sensitive to identification errors that may arise from various sources, including nonlinear behavior. Additionally, the presence in the system response of other modes not sufficiently excited to be captured in the identified model can contaminate the estimation of the frequencies and damping factors of the modes of interest.

Finally, in terms of damping factors, all partners predicted low values, as expected since aerodynamics is not included. Partner Polimi, applying system identification-based stability assessment, often predicted higher values of damping. This may be partially attributed to possible numerical damping introduced in the integration scheme of the simulation.

Figures 5 and 6 display the Campbell diagram of the entire turbine considering the aerodynamics, using the wind speed as the independent variable. All plots are arranged as in Sec. 3.2. Out-of-plane modes are omitted, as they are typically associated with high damping.

Due to the complexity of the analysis, a limited number of partners provided the results. However, some interesting comments can still be derived. First, the damping factor of the

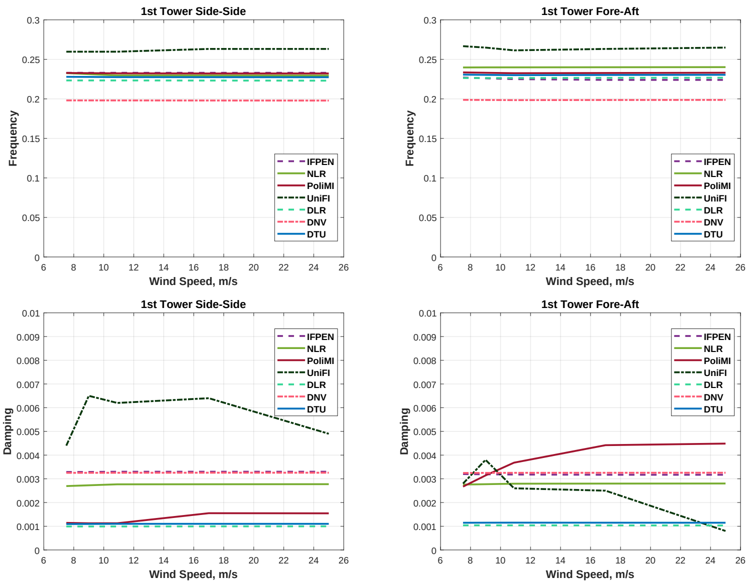

Figure 3. Campbell diagram of the tower modes in vacuo. Upper plots: frequencies; Bottom plots: damping. The name of the mode is displayed in the title of each plot.

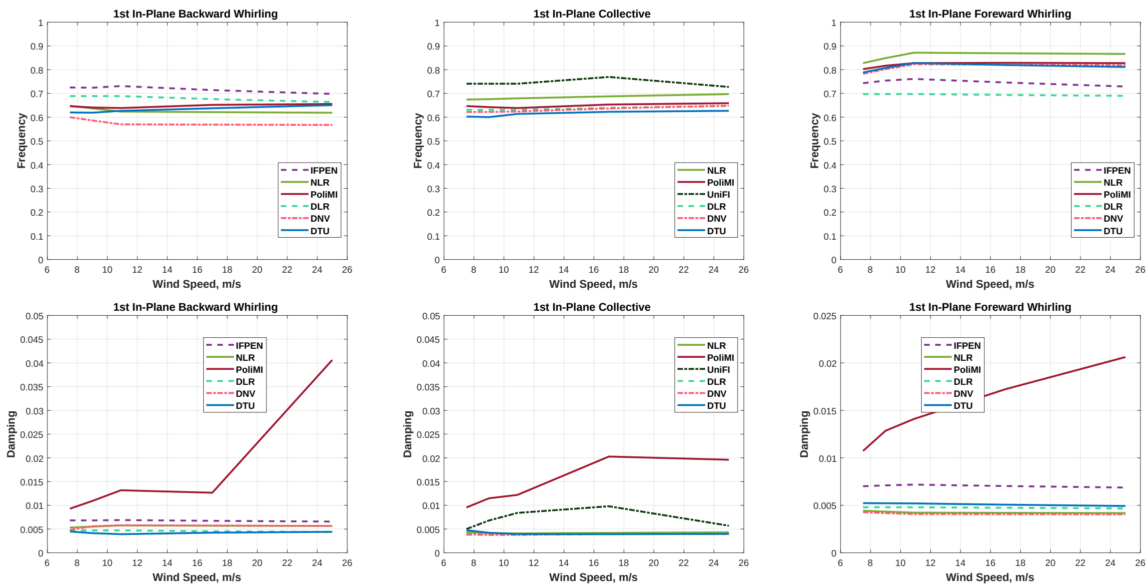

Figure 4. Campbell diagram of the in-plane modes in vacuo. Upper plots: frequencies; Bottom plots: damping. The name of the mode is displayed in the title of each plot.

tower fore-aft mode is ten times greater than that of the tower side-side mode, due to a higher aerodynamic damping. There is a mild decrease in the frequency of the collective IP (drive train) mode as the wind increases, as predicted by most partners.

A general increase in the damping of tower and in-plane modes, as the wind increases beyond 17 m/s, was predicted by all partners. In-plane modes feature a small drop in damping values around the rated speed or immediately after. More generally, the trends of the damping factors are different, but the average damping values of the low-damped modes are of similar magnitude.

By examining the damping ratios, one may quantify the spread in the estimation in terms

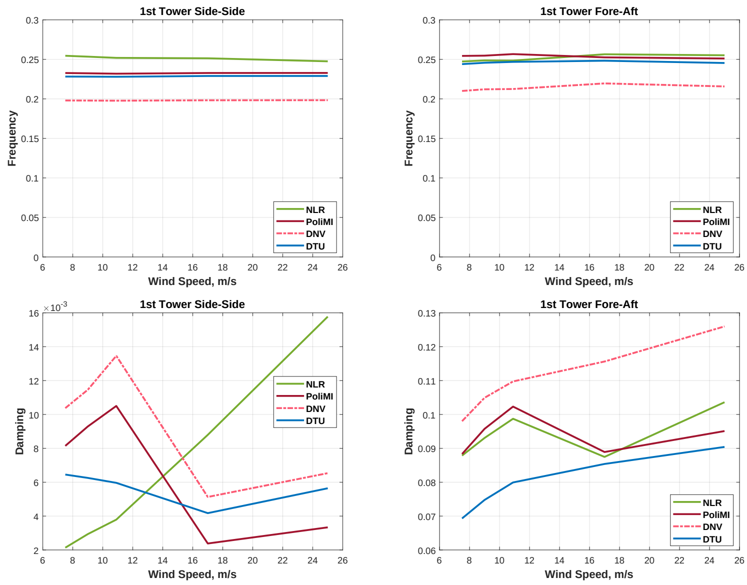

Figure 5. Campbell diagram of the tower modes of the wind turbine in air. The name of the mode is displayed in the title of each plot.

of the difference between the minimum and maximum values. This analysis, which is not fully reported in this paper for the sake of brevity, shows that this difference is roughly of the same order of magnitude as the average damping values estimated by the partners.

Since the eigenvalues do not depend linearly on the system damping, the aerodynamic contribution cannot be isolated. As a very first approximation, it can be estimated by subtracting the damping in vacuo from that in air. On average, aerodynamic and structural damping are comparable for the tower side–side and forward whirling in-plane modes, roughly twice as large for the collective in-plane mode, three times larger for the backward whirling in-plane mode, and about an order of magnitude larger for the tower fore–aft mode. This stresses even more the importance of selecting adequate structural damping values when modeling wind turbines.

3.3. Nominal Wind Profile (NWP) simulations

Full aero-elastic models have finally been used for performing time simulation of the turbine subject to a steady NWP wind.

Dealing with the "*simplified*" model, the comparisons among Partners' results are shown from Fig. 7 to 9. The comparison of "*full*" model outputs, are displayed from Fig. 10 to 12. In all plots, the curves labeled "INM-MP" refer to simulations where partner INM modified the pitch to match the power according to the values reported in [8]. The agreement is reasonably good for most of the variables of interest, although the spread of the results is significant, especially in the lateral degrees of freedom, e.g. tower side-side and blade root edge-wise.

The same exercise made within the IEA Task-29 had shown a more accurate matching among the different partners' outputs[7]. Probably, the reason for such discrepancies is to be sought in the flexibility of the 15 MW RWT and in the formulation used to render the blade torsional degrees of freedom. In fact, any mismatch in the blade torsion results in variations in sectional angles of attack, which in turn may lead to significant differences in the aerodynamic forces. To provide a quantitative indication, the rotor thrust of the "full model" exhibits a spread (i.e. the ratio between standard deviation and mean value) in the range 7–23%, whereas in IEA Task-29, which considered a more rigid turbine, it was below 5% for all analyzed wind speeds.

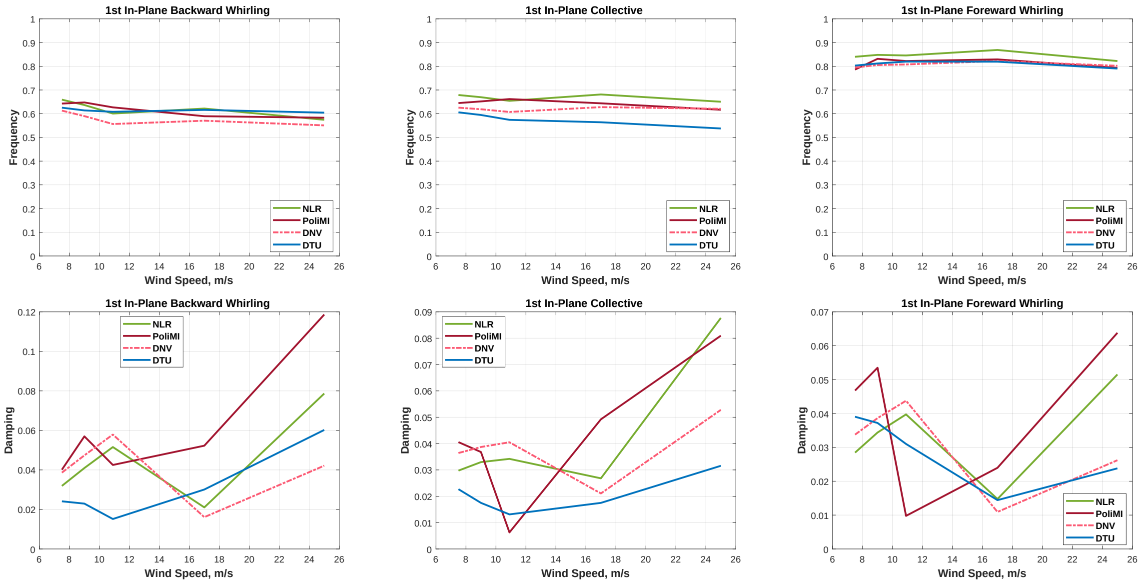

Figure 6. Campbell diagram of the in-plane modes in air. Upper plots: frequencies; Bottom plots: damping. The name of the mode is displayed in the title of each plot.

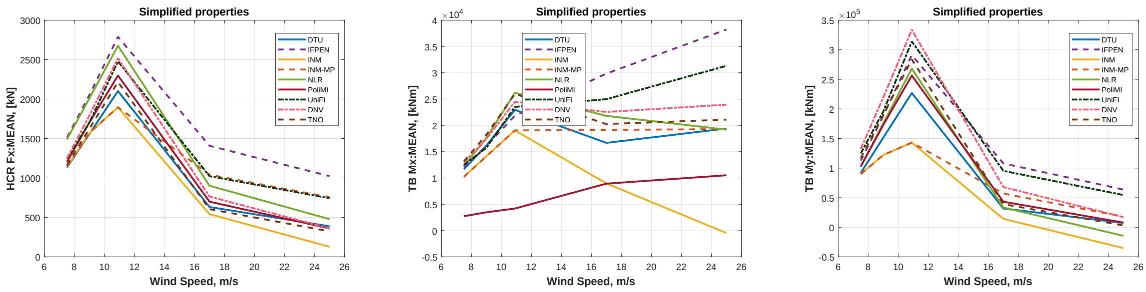

Figure 7. Non-rotating measurements of the "*simplified*" model. Left plot: thrust; center plot: side-side bending moment; right plot: fore-aft bending moment.

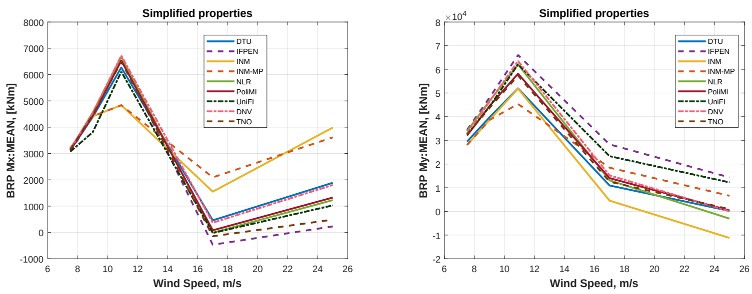

Figure 8. Blade root loads of the "*simplified*" model. Left: edge-wise bending moment; right plot: flap-wise bending moment.

4. Conclusions

From the analysis conducted in this work, several observations can be drawn. First, the different codes and analysis tools predict with reasonable accuracy the modal characteristics of the wind turbine subcomponents. In terms of blade frequency, the agreement in the predictions is

Journal of Physics: Conference Series **3224** (2026) 042028 doi:10.1088/1742-6596/3224/4/042028

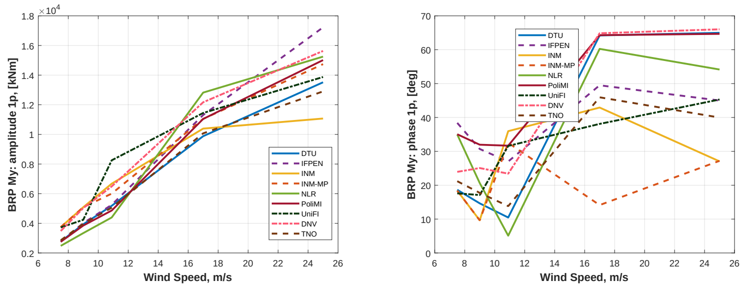

Figure 9. 1p blade root flap-wise load of the "*simplified*" model. Left: amplitude; right plot: phase.

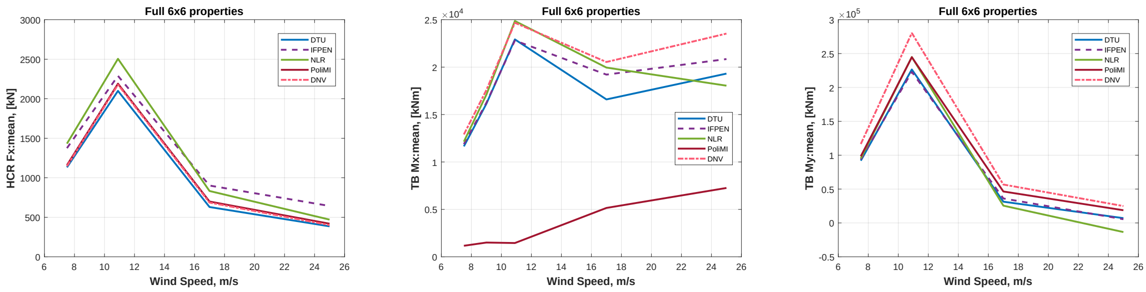

Figure 10. Non-rotating measurements of the "*full*" model. Left plot: thrust; center plot: side-side bending moment; right plot: fore-aft bending moment.

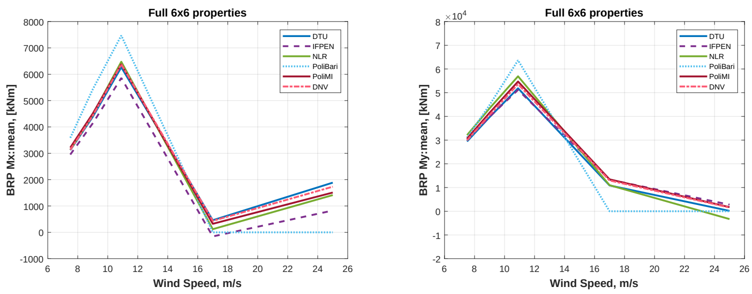

Figure 11. Blade root loads of the "*full*" model. Left: edge-wise bending moment; right plot: flap-wise bending moment.

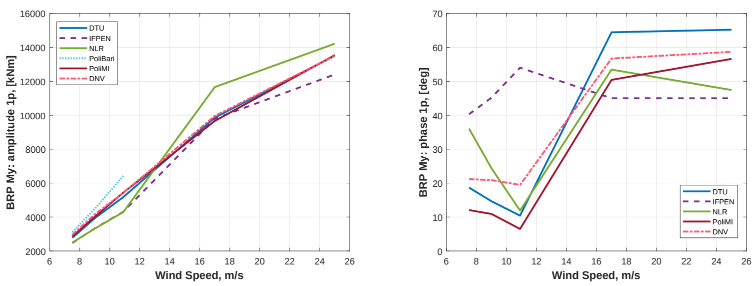

Figure 12. 1p blade root flap-wise load of the "*full*" model. Left: amplitude; right plot: phase.

extremely satisfactory for the lowest modes, which mostly influence the relevant turbine response. Damping factors estimation is more affected by the details of the blade model implementation inside the simulation codes, i.e. modal condensation versus sectional damping proportional to the stiffness. This fact is reflected in the higher level of spread. The torsional mode, on the other hand, features a higher level of spread among the results of all partners. The reason lies in the different implementations of the torsional degrees of freedom in the simulation tools.

The agreement in the partners' predictions of the frequencies of the entire turbine in vacuo and in the air is reasonably good, with damping factors featuring a higher level of spread.

The comparison of the output in the NWP dynamic simulations shows a reasonably good match. However, the level of spread is higher than that obtained during a similar exercise conducted within the IEA Task-29 with a smaller and more rigid turbine [7]. Most probably, the flexibility of this turbine is responsible for the discrepancy.

Acknowledgments
This work was carried out within the framework of the IEA Wind TCP Task 47 (TURBINIA). This work was authored in part by the National Laboratory of the Rockies for the U.S. Department of Energy (DOE), operated under Contract No. DE-AC36-08GO28308. Funding provided by U.S. Department of Energy Office of Energy Efficiency and Renewable Energy Wind Energy Technologies Office. The views expressed in the article do not necessarily represent the views of the DOE or the U.S. Government. The U.S. Government retains and the publisher, by accepting the article for publication, acknowledges that the U.S. Government retains a nonexclusive, paid-up, irrevocable, worldwide license to publish or reproduce the published form of this work, or allow others to do so, for U.S. Government purposes.

References

[1] Bir G 2008 Multi-blade coordinate transformation and its application to wind turbine analysis *AIAA Wind Energy Symposium* (Reno, Nevada)

[2] Hansen M H 2004 Aeroelastic stability analysis of wind turbines using an eigenvalue approach *Wind Energy* **7** 133–143

[3] Bottasso C and Cacciola S 2015 Model-independent periodic stability analysis of wind turbines *Wind Energy* **18** 865–887

[4] Skjoldan P F and Hansen M H 2012 Implicit floquet analysis of wind turbines using tangent matrices of a non-linear aeroelastic code *Wind Energy* **15** 275–287

[5] Collier W, Ors D, Barlas T, Zahle F, Bortolotti P, Marten D, Jensen C S L, Branlard E, Zalkind D and Lønbæk K 2024 Aeroelastic code comparison using the iea 22mw reference turbine *Journal of Physics: Conference Series* **2767** 052042

[6] Schepers J G *et al* 2025 Turbinia, turbulent inflow innovative aerodynamics Tech. rep. IEA Wind TCP - Task 47

[7] Schepers J G *et al* 2021 IEA Wind TCP Task 29, Phase IV: Detailed Aerodynamics of Wind Turbines Zenodo URL `https://doi.org/10.5281/zenodo.4925963`

[8] Gaertner E *et al* 2020 Definition of the iea 15-megawatt offshore reference wind turbine Tech. rep. International Energy Agency

[9] Germanischer Lloyd Industrial Services GmbH 2010 Guideline for the certification of wind turbines. Tech. rep. Germanischer Lloyd Industrial Services GmbH Hamburg, Germany

[10] Bittanti S and Colaneri P 2009 *Periodic Systems: Filtering and Control* 1st ed Communications and Control Engineering (Springer London) ISBN 978-1-84800-911-0